# MODELING, DESIGN AND EXPERIMENTAL CHARACTERIZATION OF THE Q-BAND OMTS AND POLARIZERS FOR THE STRIP-LSPE BALLOON EXPERIMENT

Oscar Antonio Peverini (1), Giuseppe Virone (1), Giuseppe Addamo (1), Mauro Lumia (1), Zunnoorain Farooqui (1), Riccardo Tascone (1), Aniello Mennella (2), Marco Bersanelli (2), Gianluca Morgante (3), Mario Zannoni (4), Massimo Gervasi (4), Anna Gregorio (5), Andrea Zacchei (6),

(1) IEIIT-CNR, c/o Politecnico di Torino, C.so Duca degli Abruzzi 24, 10129 Torino, Italy,
Email: oscar.peverini@ieiit.cnr.it
(2) Dipartimento di Fisica, Università degli Studi di Milano, via Celoria, 16, 20133 Milano, Italy
(3) INAF-IASF Bologna, via Gobetti 101, 40129 Bologna, Italy
(4) Dipartimento di Fisica, Università di Milano - Bicocca, P.zza della Scienza 3, 20126 Milano, Italy
(5) Dipartimento di Fisica - Università di Trieste, via Valerio 2, 34127 Trieste, Italy
(6) INAF Osservatorio Astronomico di Trieste, via G.B. Tiepolo 11, 34131 Trieste, Italy

ABSTRACT

This paper reports on the Q-band polarizers and ortho-mode transducers developed for the STRatospheric Italian Polarimeter (STRIP) coherent multi-feed instrument. A split-block design of groove polarizers and an ad-hoc assembly procedure have been conceived in order to achieve recurring high-performance for all the 49 polarizers (*i.e.*, cross-polarization < -35 dB, return-loss > 36 dB, insertion-loss < 0.07 dB). The ortho-mode transducers are based on a novel multi-layer turnstile-junction design. This configuration has been conceived toward a high parallelization rate of the manufacturing process, while providing high electromagnetic performance (cross-coupling < -50 dB, isolation > 50 dB).

## 1. INTRODUCTION

The Large Scale Polarization Explorer (LSPE) is a balloon-based experiment funded by the Italian Space Agency aimed at the measurement of the Cosmic Microwave Background (CMB) polarization state at large angular scales. The LSPE experiment will embark two instruments: the STRatospheric Italian Polarimeter (STRIP) [1] consisting of an array of 49 coherent receivers operating in the Q-band, and the Short Wavelength Instrument for the Polarization Explorer (SWIPE) [2] based on bolometric detectors operating from 140 GHz to 240 GHz.

Since high instrumentation sensitivity is needed in order to detect the very faint levels of the B-modes (< 1μK), the LSPE-STRIP instrument is based on the simultaneous detection of the *Q* and *U* Stokes parameters of the incoming radiation through an array of 49 correlation receivers operating from 39 GHz to 48 GHz (20% bandwidth). The receiver array will consist of 7 hexagonal modules, each one containing seven receivers elements (see Fig. 1), placed in the focal plane of a Dragonian side-fed dual reflector telescope and will be enclosed in a 20K helium cryostat.

## 2. LSPE-STRIP RECEIVER ARCHITECTURE

The operation of each receiver is based on the measurement of the correlation between the Right- and Left-Hand Circular Polarization (RHCP and LHCP) components of the electromagnetic signal according to

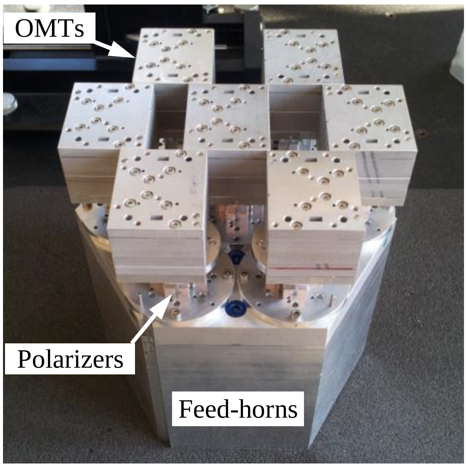


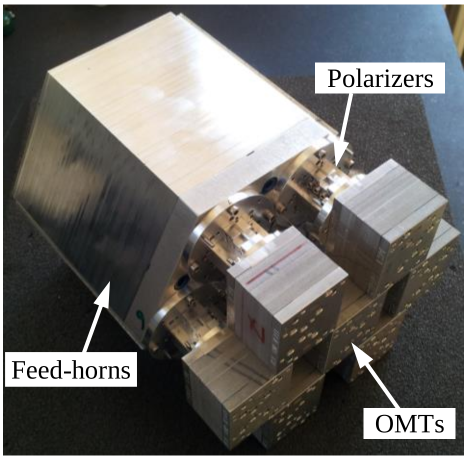


Figure 1. Q-band hexagonal antenna-feed module.

the Stokes parameter definition

$$Q = < |E_x|^2 - |E_y|^2 > = < 2\mathrm{Re}\{AB^*\} >$$

$$U = < 2\mathrm{Re}\{E_x E_y^*\} > = < 2\mathrm{Im}\{AB^*\} >$$

$$V = < -2\mathrm{Im}\{E_x E_y^*\} > = < |B|^2 - |A|^2 > \quad (1)$$

$$I = < |E_x|^2 + |E_y|^2 > = < |A|^2 + |B|^2 >,$$

where $A$ and $B$ denote the RHCP and LHCP components, and the symbol <…> represents the spectral average in the working band. The schematic of the receiver architecture is shown in Fig. 2. The RHCP and LHCP components are collected through the corrugated horn and routed to the polarizer. The latter converts the two circular polarizations in two linearly polarized signals oriented along the main axes of the ortho-mode transducer (OMT). To this aim, the polarizer principal-axes L and C are rotated by 45 deg with respect to the OMT axes. The two linearly polarized signals are, hence, extracted from the common waveguide through the OMT and routed to the correlation unit. The latter is a Monolithic Microwave Integrated Circuit (MMIC) based on the design developed for the QUIET experiment [3]. According to the layout reported in [1], the correlation unit integrates six low-noise HEMT amplifiers, two phase switches, a 180-deg hybrid coupler, two power-splitters, four band-pass filters, a 90-deg hybrid coupler and four diode detectors. The chip provides four output voltages that are proportional to the sum and difference, in phase and in quadrature, of the input RF signals $A$ and $B$

$$V_{\mathrm{D1}} \propto < |A+B|^2 >$$

$$V_{\mathrm{D2}} \propto < |A-B|^2 >$$

$$V_{\mathrm{D3}} \propto < |A+jB|^2 > \quad (2)$$

$$V_{\mathrm{D4}} \propto < |A-jB|^2 >.$$

Hence, the Stokes parameters $Q$ and $U$ are detected as

$$Q_m \propto V_{\mathrm{D1}} - V_{\mathrm{D2}} \quad (3)$$

$$U_m \propto V_{\mathrm{D3}} - V_{\mathrm{D4}}.$$

In order to identify the best polarizer and ortho-mode transducer designs for the LSPE-STRIP correlation receivers, the electromagnetic behaviour of these components have been described in terms of the Muller matrix $\boldsymbol{M}$ relating the input and output Stoke parameters

$$\begin{bmatrix} Q \\ U \\ V \\ I \end{bmatrix}_{\mathrm{out}} = \boldsymbol{M} \cdot \begin{bmatrix} Q \\ U \\ V \\ I \end{bmatrix}_{\mathrm{in}} = \begin{bmatrix} \boldsymbol{H} & \boldsymbol{K} \\ \boldsymbol{P} & \boldsymbol{N} \end{bmatrix} \cdot \begin{bmatrix} Q \\ U \\ V \\ I \end{bmatrix}_{\mathrm{in}}. \quad (4)$$

Since the LSPE-STRIP instrument is designed to measure the Stokes parameters $Q$ and $U$**,** the relevant blocks of the Muller matrix $\boldsymbol{M}$ are the sub-matrices $\boldsymbol{H}$ and $\boldsymbol{K}$ defining the relationship

$$\begin{bmatrix} Q \\ U \end{bmatrix}_{\mathrm{out}} = \begin{bmatrix} H_{QQ} & H_{QU} \\ H_{UQ} & H_{UU} \end{bmatrix} \cdot \begin{bmatrix} Q \\ U \end{bmatrix}_{\mathrm{in}} + \begin{bmatrix} K_{QV} & K_{QI} \\ K_{UV} & K_{UI} \end{bmatrix} \cdot \begin{bmatrix} V \\ I \end{bmatrix}_{\mathrm{in}}. \quad (5)$$

The most demanding requirements set on the LSPE-STRIP receivers involve the coefficients $K_{QI}$ and $K_{UI}$. These coefficients define the spurious leakage of the total intensity $I$ in the $Q$ and $U$ channels. Indeed, $I$ contains both the polarized and unpolarised CMB components and the instrument noise referred at the antenna section, and, hence, it is several orders of magnitude higher than the $Q$ and $U$ linearly polarized components to be detected.

In the following, the modelling, the design and the experimental characterization of the Q-band polarizer and OMT modules developed for the LSPE-STRIP instrument are reported.

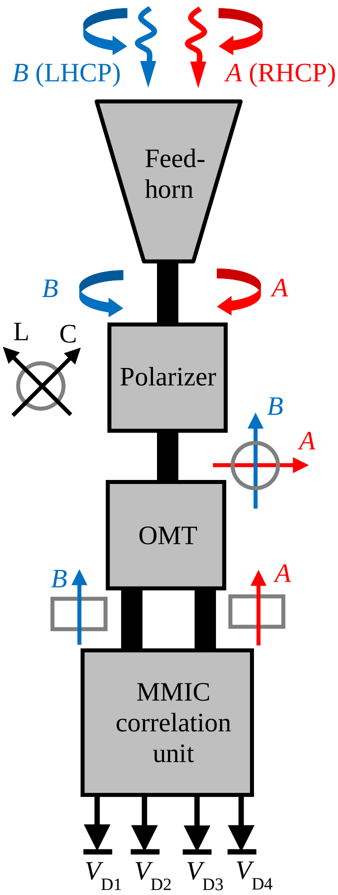


Figure 2. Schematic of the Q-band dual-polarization correlation receiver of the LSPE-STRIP instrument. L and C denote the inductive and capacitive principal polarizer axes.

Table 1. Measured electromagnetic performance of the 49 Q-band polarizers.

| Parameter | Measured value |
|---|---|
| Return loss | $\geq$ 36 dB |
| Insertion loss | $\leq$ 0.07 dB |
| Insertion-loss equalization | $\leq$ 0.01 dB |
| Phase-difference deviation from 90 deg | $\leq$ 2.0 deg |
| Cross-polarization | $\leq$ -35 dB |

## 3. POLARIZERS

In order to derive the blocks ***H*** and ***K*** of the polarizer Muller matrix (4), the 2 x 2 transmission block of the polarizer scattering matrix is considered

$$\boldsymbol{S}^{(2,1)} = \begin{bmatrix} T_{\mathrm{LL}} & T_{\mathrm{LC}} \\ T_{\mathrm{CL}} & T_{\mathrm{CC}} \end{bmatrix} \quad (6)$$

where L and C denote the inductive and capacitive principal polarizer axes. Hence, the following expressions can be derived

$$\begin{aligned} H_{QQ} &= \frac{1}{2}\{|T_{\mathrm{LL}}|^2 + |T_{\mathrm{CC}}|^2 - |T_{\mathrm{LC}}|^2 - |T_{\mathrm{CL}}|^2\} \\ H_{QU} &= \mathrm{Re}\{T_{\mathrm{LL}}T_{\mathrm{LC}}^* - T_{\mathrm{CL}}T_{\mathrm{CC}}^*\} \\ H_{UQ} &= \mathrm{Im}\{T_{\mathrm{LL}}T_{\mathrm{CL}}^* - T_{\mathrm{LC}}T_{\mathrm{CC}}^*\} \\ H_{UU} &= \mathrm{Im}\{T_{\mathrm{LC}}T_{\mathrm{CL}}^* + T_{\mathrm{LL}}T_{\mathrm{CC}}^*\} \end{aligned} \quad (7)$$

and

$$\begin{aligned} K_{QI} &= \frac{1}{2}\{|T_{\mathrm{LL}}|^2 - |T_{\mathrm{CL}}|^2 + |T_{\mathrm{LC}}|^2 - |T_{\mathrm{CC}}|^2\} \\ K_{QV} &= \mathrm{Im}\{T_{\mathrm{LL}}T_{\mathrm{LC}}^* - T_{\mathrm{CL}}T_{\mathrm{CC}}^*\} \\ K_{UI} &= \mathrm{Im}\{T_{\mathrm{LL}}T_{\mathrm{CL}}^* + T_{\mathrm{LC}}T_{\mathrm{CC}}^*\} \\ K_{UV} &= \mathrm{Re}\{T_{\mathrm{LC}}T_{\mathrm{CL}}^* - T_{\mathrm{LL}}T_{\mathrm{CC}}^*\}. \end{aligned} \quad (8)$$

Under the assumption (experimentally verified) that the selected manufacturing process introduce very weak cross-couplings between the principal polarizations (*i.e.* $T_{\mathrm{LC}} = T_{\mathrm{LC}} \approx 0$) Eqs. 7-8 simplify as

$$\begin{aligned} H_{QQ} &= \frac{1}{2}\{|T_{\mathrm{LL}}|^2 + |T_{\mathrm{CC}}|^2\} \\ H_{QU} &= H_{UQ} = 0 \\ H_{UU} &= \mathrm{Im}\{T_{\mathrm{LL}}T_{\mathrm{CC}}^*\} \end{aligned} \quad (9)$$

and

$$\begin{aligned} K_{QI} &= \frac{1}{2}\{|T_{\mathrm{LL}}|^2 - |T_{\mathrm{CC}}|^2\} \\ K_{QV} &= K_{UI} = 0 \\ K_{UV} &= -\mathrm{Re}\{T_{\mathrm{LL}}T_{\mathrm{CC}}^*\}. \end{aligned} \quad (10)$$

It can be easily inferred from Eqs. 9-10 that any deviation of the phase difference between the two

Table 2. Measured coefficients of the blocks ***H*** and ***K*** of the Mueller matrix (4).

| | Polarizer | OMT | Polarizers + OMTs sub-assemblies |
|---|---|---|---|
| Sub-matrix ***H*** | | | |
| $H_{QQ}$ | $\geq$ 0.06 dB | $\geq$ 0.6 dB | $\geq$ 0.7 dB |
| $H_{QU}$ | - | $\leq$ -15 dB | $\leq$ -14 dB<br>$\leq$-20 dB with shim and post-processing |
| $H_{UQ}$ | - | $\leq$ -15 dB | $\leq$ -14 dB<br>$\leq$-20 dB with shim and post-processing |
| $H_{UU}$ | $\geq$ 0.06 dB | $\geq$ 0.6 dB | $\geq$ 0.7 dB |
| Sub-matrix ***K*** | | | |
| $K_{QV}$ | - | $\leq$ -28 dB | $\leq$ -17 dB |
| $K_{QI}$ | $\leq$ -25 dB | $\leq$ -29 dB | $\leq$ -25 dB |
| $K_{UV}$ | $\leq$ -15 dB | $\leq$ -23 dB | $\leq$ -15 dB |
| $K_{UI}$ | - | $\leq$ -30 dB | $\leq$ -30 dB |

principal-polarization transmission coefficients from theoretical value of 90 deg leads to a loss in the detected *U* parameter and a leakage of the Stoke parameter *V* in the *U* channel . Even more essential is the minimization of the insertion loss difference between the two principal-polarization transmissions, since it leads to a total intensity leakage in the *Q* channel. In order to meet the aforesaid requirements at affordable costs, a groove polarizer based on a split-block layout has been designed. All the grooves are realized in two comb plates [4] of constant thickness *s*. The depth of the grooves and the height of the waveguide ridges between the grooves have been defined according to an optimum-set procedure similar to that reported in [5]. The polarizer consists of six mechanical parts that have been accurately aligned through an ad-hoc assembling procedure based on the use of Johansson gauges.

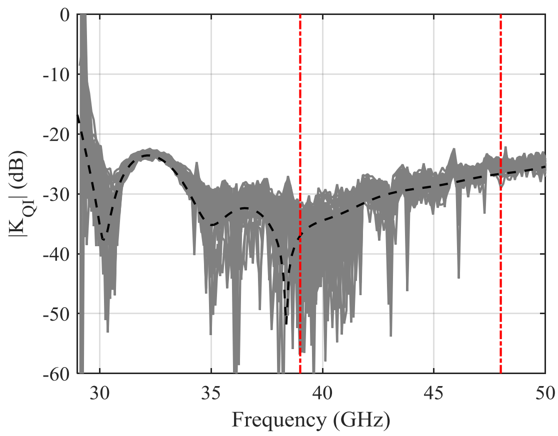


Figure 3. Measured values of the coefficient $K_{QI}$ (5) for the 49 Q-band polarizers. The predicted performance are reported in black dashed line. The vertical red bars denote the working band [39, 48] GHz.

Figure 4. Al-alloy OMT plates manufactured through wire EDM.

This procedure has also allowed for a fine tuning of the comb plates in order to compensate for the manufacturing uncertainties (< 0.02 mm). Two prototypes with different comb plate thickness ($s$ equal to 1.5 and 3.0 mm) have previously been machined and tested. Subsequently, on the basis of the selected layout, all the 49 flight units have been manufactured and tested at room temperature in the principal-polarization basis. Table 1 reports the measured electromagnetic performance of the 49 Q-band polarizers. The corresponding measured values of the blocks $\boldsymbol{H}$ and $\boldsymbol{K}$ of the Muller matrix are listed in the second column of Tab. 2. Since the cross-coupling transmissions in the polarization-basis have been experimentally assessed to be lower than the test-bench de-polarization systematic error (in the order of -50 dB), the measured values reported in Tab. 2 refer to Eqs. 9-10. It has to be remarked that the total intensity leakage in the $Q$ channel ($K_{QI}$) is lower than -25 dB in the working band, as reported in Fig. 3.

## 4. ORTHO-MODE TRANSDUCERS

The Muller matrix has been derived also toward the definition of the best OMT design for the LSPE-STRIP correlation receivers. By considering the 2 x 2 transmission block of the OMT scattering matrix in the linear polarization basis (see Fig. 2)

$$\boldsymbol{S}^{(2,1)} = \begin{bmatrix} T_{AA} & T_{AB} \\ T_{BA} & T_{BB} \end{bmatrix}, \tag{11}$$

the following expressions for the elements of the sub-matrices $\boldsymbol{H}$ and $\boldsymbol{K}$ can be derived

$$\begin{aligned} H_{QQ} &= \mathrm{Re}\{T_{AA}T_{BB}^* + T_{AB}T_{BA}^*\} \\ H_{QU} &= -\,\mathrm{Im}\{T_{AA}T_{BB}^* - T_{AB}T_{BA}^*\} \\ H_{UQ} &= \mathrm{Im}\{T_{AA}T_{BB}^* + T_{AB}T_{BA}^*\} \\ H_{UU} &= \mathrm{Re}\{T_{AA}T_{BB}^* - T_{AB}T_{BA}^*\} \end{aligned} \tag{12}$$

and

$$\begin{aligned} K_{QI} &= \mathrm{Re}\{T_{AA}T_{BA}^* + T_{AB}T_{BB}^*\} \\ K_{QV} &= \text{-}\mathrm{Re}\{T_{AA}T_{BA}^* - T_{AB}T_{BB}^*\} \end{aligned}$$

Table 3. Measured electromagnetic performance of the 49 Q-band OMTs.

| **Parameter** | **Measured value** |
|---|---|
| Return loss | ≥ 22 dB |
| Insertion loss | ≤ 0.6 dB |
| Isolation | ≥ 50 dB |
| Cross-polarization | ≤ -50 dB |

$$\begin{aligned} K_{UI} &= \mathrm{Im}\{T_{AA}T_{BA}^* + T_{AB}T_{BB}^*\} \\ K_{UV} &= -\mathrm{Im}\{T_{AA}T_{BA}^* - T_{AB}T_{BB}^*\}. \end{aligned} \tag{13}$$

Since the block $\boldsymbol{H}$ has to be as close as possible to the identity matrix, the OMT cross-polar transmission coefficients ($T_{AB}$ and $T_{BA}$) should be minimized, and the two co-polar transmission coefficients ($T_{AA}$ and $T_{BB}$) should be phase-equalized. Under these conditions, the spurious contamination matrix $\boldsymbol{K}$ is also minimized. However, it has to be noticed that the total intensity leakage terms ($K_{QI}$ and $K_{UI}$**)** affecting the $Q$ and $U$ OMT channels depend on the term

$$T_{AA}T_{BA}^* + T_{AB}T_{BB}^*. \tag{14}$$

It can be easily proved that this quantity is ideally zero for a perfectly-matched loss-less OMT. Hence, high values of OMT return-loss reduce the spurious contamination due to the total intensity.

On the basis of these electromagnetic requirements, the turnstile-junction symmetric OMT reported in details in [6] has been designed. This configuration is particularly suitable for the medium-scale production of high-performance OMTs used in multi-feed dual-polarization instrumentation aimed at astrophysical and radio-astronomical surveys. Indeed, only standard-thickness Al plates have been used, and wire electrical-discharge machining (EDM) of stacks consisting of identical plates has allowed for manufacturing parallelization. Figure 4 shows some of the Al-alloy plates manufactured through wire EDM. In order to identify the best material, the electrical resistivity of different standard-thickness metal layers has been measured both at room- and at cryogenic temperature. On the basis of the select Al-alloy, five OMT prototypes have been preliminarily manufactured and tested. In particular, the prototypes have undergone thermal cycles down to 15 K in order to assess their compliance to operation in cryogenic environment. Subsequently, all the 49 OMT flight units have been developed and accurately measured through the full dual-polarization procedure reported in [7].

Figure 5 shows the measured return loss (a), insertion-loss (b) and cross-couplings (c) of the Q-band OMT cluster, whereas Table 3 summarizes the measured electrical performance. The measured coefficients of the Muller matrix blocks $\boldsymbol{H}$ and $\boldsymbol{K}$ are listed in the third column of Tab. 2. It can be noticed that levels lower

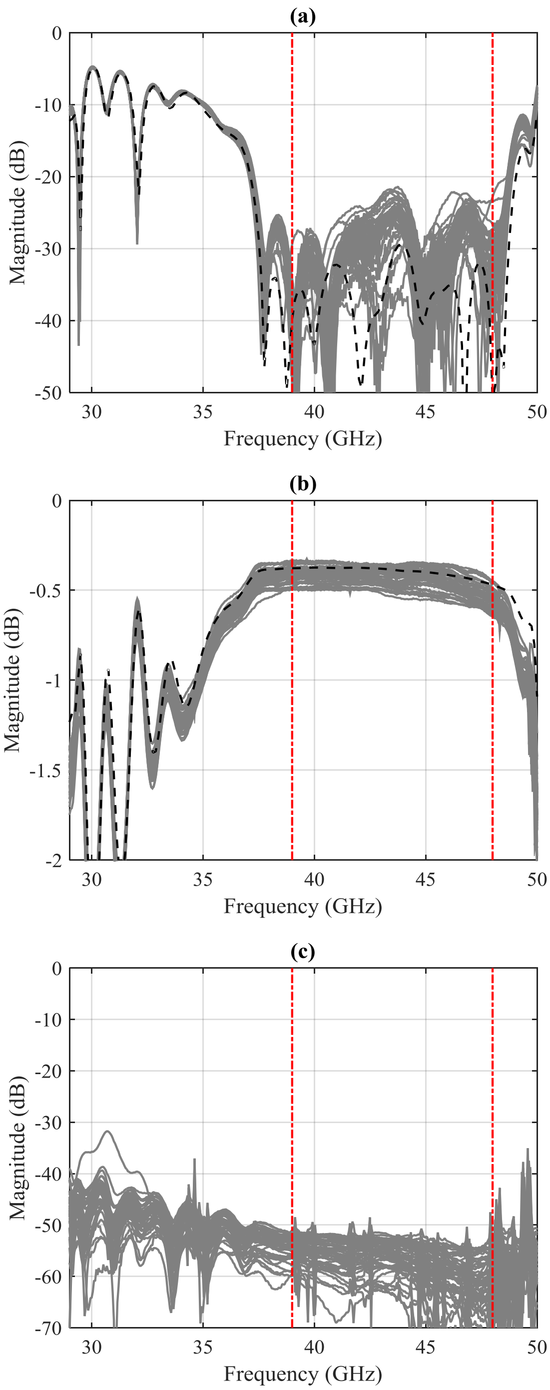


Figure 5. Measured scattering parameters of the 49 Q-band OMTs. The predicted performance are reported in black dashed line. The vertical red bars denote the working band [39, 48] GHz.
(a) Reflection coefficient at the rectangular WR22 ports. (b) Co-polar transmission and (c) cross-polar transmission coefficients from the rectangular ports to the linear polarizations propagating in the common circular waveguide.

than approximately -30 dB have been achieved for spurious leakage coefficients $K_{QI}$ and $K_{UI}$.

Table 4. Measured electromagnetic performance of the 49 sub-assemblies consisting of the Q-band polarizers and OMTs.

| Parameter | Measured value |
|---|---|
| Return loss | ≥ 22 dB |
| Insertion loss | ≤ 0.7 dB |
| Isolation | ≥ 40 dB |
| Cross-polarization | ≤ -35 dB |

## 5. POLARIZERS AND ORTHO-MODE TRANSDUCERS SUB-ASSEMBLIES

The 49 Q-band sub-assemblies consisting of polarizers and OMTs have been mounted and measured at room temperature. Figure 6 shows the measured values for the return loss at the rectangular WR22 ports (to be connected to the MMIC correlation units) (a), the isolation between the rectangular ports (b), and the cross-polar transmission coefficients from the input circular waveguide port (to be connected to the feed-horn) to the rectangular WR22 ports (c). Table 4 lists all the relevant electromagnetic performance of the 49 sub-assemblies. On the basis of the measured scattering matrices, the blocks $\boldsymbol{H}$ and $\boldsymbol{K}$ of the Mueller matrix relating the input and output Stokes parameters have been evaluated. To this end, it has to be remarked that (12) and (13) also hold for the sub-assemblies composed of polarizers and OMTs. It has been verified that the corresponding values well fit with those obtained by cascading the measured Mueller matrices of the single components. The fourth column in Table 2 reports all the coefficients of the sub-matrices $\boldsymbol{H}$ and $\boldsymbol{K}$, whereas the direct terms $H_{QQ}$ and $H_{UU}$ and the most demanding spurious terms $K_{QI}$ and $K_{UI}$ are reported as a function of frequency in Fig. 7. It can be noticed that rejection levels to the total intensity $I$ of approximately 25 dB and 30 dB have been achieved for the $Q$ and $U$ channels, respectively. The values of the coefficients $K_{QV}$ and $K_{UV}$ are instead in the order of -15 dB. Since the Stokes parameters are quadratic quantities, the values of $K_{QV}$ and $K_{UV}$ are commensurate with the cross-coupling levels of approximately -35 dB that are provided by the sub-assemblies (mainly by the polarizers). The lower values achieved for the coefficients $K_{QI}$ and $K_{UI}$ arise from an adequate fulfilment of the loss-less and matching condition (14). It has also to be remarked that the off-diagonal entries of matrix $\boldsymbol{H}$ can be minimized through a befitting shimming (in the order of 0.01-0.05 mm) of the output WR22 ports and through an off-line rotation of the detected coefficients in the $Q$ - $U$ plane.

## ACKNOWLEDGMENTS

This work has been carried out in the context of the ASI programme “Large Scale Polarization Experiment (LSPE)” (contract I/022/11/0).

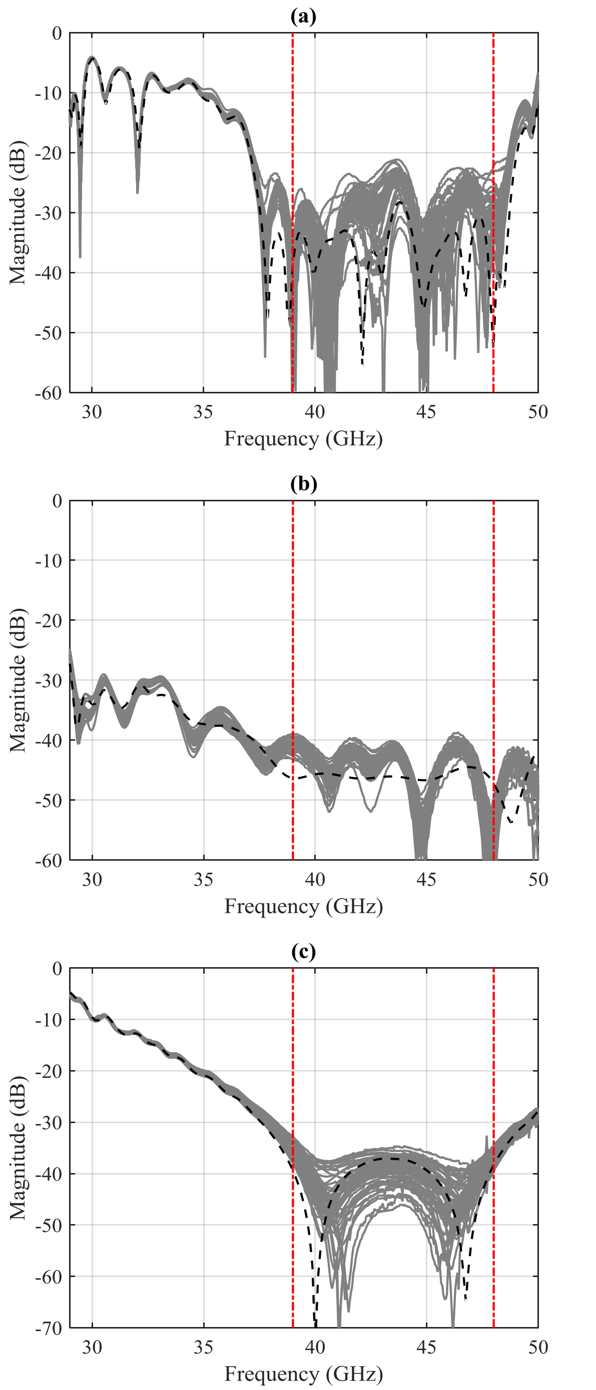


Figure 6. Measured scattering parameters of the 49 sub-assemblies composed of polarizers and OMTs. The simulated design curves are reported in black dashed line. The vertical red bars denote the working band [39, 48] GHz.
(a) Reflection coefficient at the rectangular WR22 ports to be connected to the MMIC polarimetric units.
(b) Isolation between the rectangular ports.
(c) Cross-polar transmission coefficient from the rectangular ports to the circular polarizations propagating in the circular waveguide.

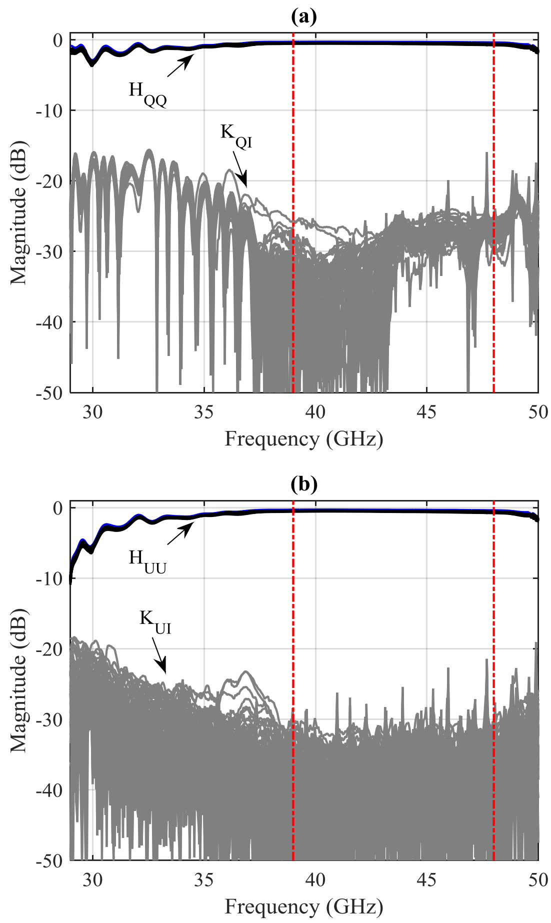


Figure 7. Measured values of the coefficients $H_{QQ}$, $H_{UU}$, $K_{QI}$ and $K_{UI}$ (5) relating the Stokes parameters at the input and output ports of the 49 polarizer + OMT assemblies. The vertical red bars denote the working band [39, 48] GHz.
(a) Q channel.
(b) U channel.

## 6. REFERENCES

[1] M. Bersanelli, *et al.*, "A coherent polarimeter Array for the Large Scale Polarization Explorer (LSPE) balloon experiment", *in Proc. of the SPIE Conference Astronomical Telescopes + Instrumentation 2012*, Amsterdam, The Netherlands, July 2012.

[2] P. De Bernardis, *et al.*, "SWIPE: a bolometric polarimeter for the Large-Scale Polarization Explorer", *in Proc. of the SPIE Conference Astronomical Telescopes + Instrumentation 2012*, Amsterdam, The Netherlands, July 2012.

[3] QUIET Collaboration, "The Q/U imaging experiment instrument", *The Astrophysical Journal*, vol. 768, no 1, May 2013.

[4] S. Y. Eom, and Y. B. Korchemkin, "A New comb circular polarizer suitable for millimeter-band

application", *ETRI Journal*, vol. 28, no. 5, pp. 656-659, Oct. 2006.

[5] G. Virone, *et al*., "Optimum-Iris-Set Concept for Waveguide Polarizers", *IEEE Microwave and Wireless Components Letters*, vol. 17, no. 3, pp. 202-204, March 2007.

[6] G. Virone, *et al*., "Platelet orthomode transducer for Q-band correlation polarimeter clusters", *IEEE Trans. on Microw. Theory Techn.*, vol. 62, no. 7, pp.1487-1493, July 2014.

[7] O. A. Peverini, *et al*., "A Microwave measurement procedure for a full characterization of ortho-mode transducers", *IEEE Trans. on Microw. Theory Tech.*, vol. 51, no. 4, pp. 1207 - 1213, April 2003.